New N-RAP-binding partners α-actinin, filamin and Krp1 detected by yeast two-hybrid screening: implications for myofibril assembly

Shajia Lu[1], Stefanie L. Carroll[1], Amy H. Herrera[1], Bradford Ozanne[2] and Robert Horowits[1,*]

[1]Laboratory of Muscle Biology, National Institute of Arthritis and Musculoskeletal and Skin Diseases, National Institutes of Health, Bethesda, MD 20892, USA
[2]Beatson Institute for Cancer Research, Garscube Estate, Switchback Road, Glasgow G61 1BD, UK
*Author for correspondence (e-mail: horowits@helix.nih.gov)

Accepted 11 February 2003
Journal of Cell Science 116, 2169-2178 Published by The Company of Biologists Ltd
doi:10.1242/jcs.00425

Summary

N-RAP, a muscle-specific protein concentrated at myotendinous junctions in skeletal muscle and intercalated disks in cardiac muscle, has been implicated in myofibril assembly. To discover more about the role of N-RAP in myofibril assembly, we used the yeast two-hybrid system to screen a mouse skeletal muscle cDNA library for proteins capable of binding N-RAP in a eukaryotic cell. From yeast two-hybrid experiments we were able to identify three new N-RAP binding partners: α-actinin, filamin-2, and Krp1 (also called sarcosin). In vitro binding assays were used to verify these interactions and to identify the N-RAP domains involved. Three regions of N-RAP were expressed as His-tagged recombinant proteins, including the nebulin-like super repeat region (N-RAP-SR), the N-terminal LIM domain (N-RAP-LIM), and the region of N-RAP in between the super repeat region and the LIM domain (N-RAP-IB). We detected significant α-actinin binding to N-RAP-IB and N-RAP-LIM, filamin binding to N-RAP-SR, and Krp1 binding to N-RAP-SR and N-RAP-IB. During myofibril assembly in cultured chick cardiomyocytes, N-RAP and filamin appear to co-localize with α-actinin in the earliest myofibril precursors found near the cell periphery, as well as in the nascent myofibrils that form as these structures fuse laterally. In contrast, Krp1 is not localized until late in the assembly process, when it appears at the periphery of myofibrils that appear to be fusing laterally. The results suggest that sequential recruitment of N-RAP binding partners may serve an important role during myofibril assembly.

Key words: N-RAP, α-actinin, Filamin, Krp1, Myofibril

Introduction

N-RAP is an actin binding LIM protein expressed in skeletal and cardiac muscle tissues (Luo et al., 1997). In adult mice, N-RAP is found at the longitudinal ends of striated muscles at sites of mechanical coupling between the myofibrils and the cell membrane (Luo et al., 1997). These regions are the myotendinous junctions in skeletal muscle and the intercalated disks in heart muscle, and ultrastructural data show that N-RAP co-localizes with the terminal actin bundles that link the myofibrils to the membrane in these regions (Herrera et al., 2000; Zhang et al., 2001). On the basis of the localization and binding affinities of N-RAP, we proposed that N-RAP serves as a link between the terminal actin of the myofibril and the protein complexes at the cell membrane (Luo et al., 1999; Luo et al., 1997).

N-RAP has also been implicated in the earliest steps of myofibril assembly (Carroll et al., 2001; Carroll and Horowits, 2000). Although subsequent steps are controversial, many investigators agree that the earliest myofibril precursors originate near the membrane, where α-actinin and actin assemble into I-Z-I complexes (Dabiri et al., 1997; Ehler et al., 1999; Imanaka-Yoshida et al., 1998; Rhee et al., 1994; Rudy et al., 2001). Time-lapse studies of living cardiomyocytes expressing α-actinin fused to GFP suggest that the closely spaced α-actinin beads in these structures aggregate laterally to form nascent myofibrils (Dabiri et al., 1997). Additional evidence suggests that muscle myosin may separately assemble into bipolar thick filaments that are oriented and incorporated into the nascent myofibrils by their interactions with titin filaments (Holtzer et al., 1997; Rudy et al., 2001; Schultheiss et al., 1990). Interestingly, nebulette, another protein with nebulin-related repeats, also appears to associate with myofibril precursors early during assembly; however, nebulette is expressed only in cardiac muscle and remains associated with mature Z-lines (Moncman and Wang, 1995; Moncman and Wang, 1999). In contrast, although N-RAP is found in all the myofibril precursors in cultured cardiomyocytes, it is not found in mature sarcomeres (Carroll and Horowits, 2000; Luo et al., 1997) and is expressed in both skeletal and cardiac muscle (Luo et al., 1997; Zhang et al., 2001).

N-RAP contains distinct regions that target to the cell periphery, the actin filaments, and the Z-lines when expressed as GFP-fusion proteins (Carroll et al., 2001). These regions are, respectively, the N-terminal LIM domain that binds talin in vitro (Luo et al., 1999), the C-terminal nebulin-related super repeats that bind actin and vinculin in vitro (Luo et al., 1999), and the region in between these two domains that binds muscle LIM protein (MLP) (Ehler et al., 2001) as well as actin,

although actin binding is ten fold weaker than in the super repeat region (Luo et al., 1999). Overexpression of any of these regions of N-RAP can inhibit myofibril assembly in the cultured cardiomyocytes (Carroll et al., 2001). This functional data led us to propose that N-RAP is an organizing center during the first steps of myofibril assembly, controlling the integration of α-actinin and actin to form the first premyofibril complex at the membrane (Carroll et al., 2001).

To discover more about N-RAP's functions and its involvement in myofibril assembly, we used yeast two-hybrid technology (Bartel and Fields, 1995) to screen a mouse skeletal muscle cDNA library for proteins capable of binding N-RAP in a eukaryotic cell. We found that N-RAP binds α-actinin, filamin and Krp1 in vivo and in vitro, and that filamin and Krp1 appear to associate with myofibrils during different steps of the assembly process, with implications for the molecular mechanism of myofibril assembly.

Materials and Methods

Constructing the N-RAP bait strain for yeast two-hybrid studies

Yeast two-hybrid experiments were conducted using the Invitrogen Hybrid-Hunter System (Invitrogen, Carlsbad, CA). Total RNA was isolated from adult mouse skeletal muscle and used as the template for cDNA synthesis, as previously described (Herrera et al., 2000). The N-RAP open reading frame was amplified by PCR as previously described (Carroll et al., 2001). The forward primer was 5′-CATA-TGGGAATTCTCCAAGATGAATGTGCAGGCC-3′, and the reverse primer was 5′-TCTCGAGGATCACGGCCGTGTACTTGAATGA-CC-3′; the underlined residues mark *Eco*RI and *Xho*I restriction sites for cloning. The purified PCR product and pHybLex/Zeo plasmid vector (Invitrogen) were double digested with *Eco*RI and *Xho*I, gel purified, mixed and ligated overnight at 4°C using T_4 ligase (Stratagene, La Jolla, CA). The ligated products were then transformed into Invitrogen One Shot TOP10 *Escherichia coli* cells and grown overnight on LB plates with Zeocin selection. Single colonies were amplified and plasmids were purified from the cells using the Quantum Prep Plasmid Miniprep Kit (Bio-Rad, Hercules, CA). Plasmids were partially sequenced to verify the integrity of the cloned inserts. The yeast bait strain was created by transforming the pHybLex/Zeo-N-RAP bait plasmid into L40 yeast cells (Invitrogen), which are His^-, Trp^-, Ura^+, Lys^+ and contain the His3 and LacZ reporter genes. Bait strain colonies were tested for autoactivation of the reporter genes by plating on the minimal defined medium and testing for β-galactosidase activity as detailed in the Hybrid-Hunter System instruction manual (Invitrogen). Bait strain colonies exhibiting no autoactivation were selected for use in subsequent experiments.

Screening for N-RAP binding partners

A cDNA library derived from mouse skeletal muscle and estimated to contain 7.2×10^6 independent clones inserted downstream of the B42 transcription activation domain in the prey vector pJG4-5 was obtained from OriGene Technologies (Rockville, MD). This library was screened for N-RAP binding partners using the Invitrogen Hybrid-Hunter yeast two-hybrid system, according to the manufacturer's protocols (Invitrogen). In brief, L40 yeast cells expressing the pHybLex/Zeo-N-RAP bait plasmid were transfected with the mouse skeletal muscle cDNA library. Assays for *LacZ* and *His3* reporter gene activities were performed according to the manufacturer's protocols (Invitrogen). Double transformants and potential binding partners were selected by 3-4 days of growth at 30°C on selective YC plates lacking uracil, lysine, tryptophan, and histidine, and including 300 μg/ml Zeocin; absence of uracil and lysine selects for the L40 yeast strain, whereas Zeocin and absence of tryptophan select for transformants carrying the pHybLex/Zeo bait plasmid and the pJG4-5 prey plasmid, respectively. Omitting histidine selects for putative binding partners by requiring activation of the *His3* reporter gene for growth. The His^+ double transformants were replica-plated for β-galactosidase activity assays.

Activation of the *lacZ* reporter gene was determined using a β-galactosidase filter lift assay as specified in the Hybrid-Hunter instruction manual (Invitrogen). Yeast colonies growing on selective media were transferred to nitrocellulose and lysed by freezing in liquid nitrogen for 1 minute. After thawing at room temperature for 1 minute, the nitrocellulose filters were placed, yeast colonies up, onto sterile Whatman #1 filter paper soaked in 1.5 ml of Z buffer (60 mM Na_2HPO_4, 40 mM NaH_2PO_4, 10 mM KCl, 1 mM $MgSO_4$, pH 7.0) containing 1 mg/ml X-gal. The filters were incubated at 30°C for 30-60 minutes; a blue color in this assay indicates strong activation of the *LacZ* reporter gene in the corresponding colony. Colonies that were positive for both histidine prototrophy and β-galactosidase activity were chosen as putative positive clones for further study.

The plasmids from initial positive clones were isolated from yeast cells using the YEASTMAKER Yeast Plasmid Isolation Kit (Clontech, Palo Alto, CA) and the cDNA inserts from all plasmids encoding candidate interacting proteins were amplified by PCR using the Advantage 2 PCR Kit (Clontech). The pJG4-5 forward (5′-GATG-CCTCCTACCCTTATGATGTGCC-3′) and reverse (5′-GGAGACTT-GACCAAACCTCTGGCG-3′) primers were used for amplifying the cDNA inserts. The following amplification cycles were utilized: 1 cycle at 95°C for 1 minute; 35 cycles at 95°C for 30 seconds then 68°C for 3 minutes; and 1 cycle at 68°C for 3 minutes. 10 μl samples of the PCR product were electrophoresed on a 0.8% agarose gel to confirm the insert for each individual clone and to verify the homogeneity of the plasmid preparation.

Aliquots of 10 μl of each amplified insert were double-digested with the frequent-cutter restriction enzymes *Alu*I and *Hae*III (Roche Diagnostics, Indianapolis, IN) in a 25 μl reaction. The digested samples were electrophoresed on Novex 4-20% polyacrylamide TBE gels (Invitrogen). Clones with identical insert sizes and restriction digest patterns were identified as probable identical clones of a single transcript, and representative clones were selected from each group for further characterization.

Plasmids from one or more representative clones from each group were transfected into One Shot TOP10 Chemically Competent *E. coli* cells (Invitrogen), amplified, and isolated using the S.N.A.P. Miniprep Kit (Invitrogen). The plasmids were reintroduced into yeast cells carrying either the pHybLex/Zeo-N-RAP bait plasmid or the negative control, the pHybLex/Zeo-Lamin bait plasmid (Invitrogen, Inc., Carlsbad, CA). The doubly transfected yeast cells were assayed for *His3* and *LacZ* reporter gene activities as detailed above. Clones resulting in specific activation of both reporter genes in the presence of pHybLex/Zeo-N-RAP but not in the presence of pHybLex/Zeo-Lamin were end-sequenced at Lofstrand Labs Limited (Gaithersburg, MD).

Antibodies

Rabbit polyclonal antibodies against N-RAP (Luo et al., 1997) and Krp1 (Spence et al., 2000) have been previously described. Polyclonal antibody against LexA was obtained from Invitrogen (Carlsbad, CA). Monoclonal antibodies against sarcomeric α-actinin, monoclonal and polyclonal antibodies against chicken gizzard filamin, and rhodamine-linked rabbit anti-mouse antibody were obtained from Sigma (St. Louis, MO). Horseradish peroxidase-linked donkey anti-rabbit and anti-mouse whole antibodies and FITC-linked donkey anti-rabbit antibody were purchased from Amersham Biosciences (Piscataway, NJ). FITC-linked donkey anti-goat ($F(ab)_2$ fragment) was purchased from Jackson Immunoresearch Laboratories (West Grove, PA).

Gel electrophoresis and immunoblotting

Single yeast colonies were grown in 5 ml of YPAD Z300 medium (YPD medium [Clontech, Palo Alto, CA] with the addition of 300 μg/ml Zeocin and 0.1 mg/ml adenine) overnight at 30°C. Cells were pelleted, washed with water, frozen on dry ice for one hour, and then mixed with 100 μl of 425-600 μm acid washed glass beads (Sigma) and 130 μl of complete cracking buffer (8 M urea, 5% SDS, 40 mM tris-HCL pH 6.8, 0.1 mM EDTA, 1% β-mercaptoethanol, 4.4 mM PMSF, 6% protease inhibitor cocktail [Sigma]); the cells were incubated at 75°C for 10 minutes and then broken by high speed vortexing for 1 minute. The cell lysate was centrifugated at 16,000 ***g*** for 5 minutes in a benchtop centrifuge. The supernatant was diluted 1:1 with 2% SDS, 20% glycerol, 140 mM β-mercaptoethanol, and 0.05% bromophenol blue. Samples were boiled for 4 minutes and 10 μg per lane was electrophoresed on a Novex NuPage 3-8% polyacrylamide tris-acetate gel (Invitrogen). After gel electrophoresis, the proteins were transblotted onto polyvinylidenedifluoride (PVDF) paper. The PVDF blots were incubated in a blocking solution of 10% non-fat dry milk and 0.2% tween-20 in phosphate buffered saline (PBS, pH 7.4) for 1 hour at room temperature. The recombinant proteins were detected by primary polyclonal antibodies against N-RAP and LexA followed by horseradish peroxidase conjugated anti-rabbit Ig; the N-RAP and LexA primary antibodies were diluted in blocking buffer 1:5000 and 1:1000, respectively, and secondary antibody was diluted in blocking buffer 1:5000. The incubations with primary antibodies were carried out at 4°C overnight and with the secondary antibody for one hour at room temperature. Bound antibodies were detected by enhanced chemiluminescence using the ECL western blotting system (Amersham Biosciences).

Bacterial expression of recombinant proteins

Three regions of mouse N-RAP (N-RAP-IB, N-RAP-LIM, N-RAP-SR) as well as chloramphenicol acetyltransferase (HIS-CAT) were expressed as N-terminal histidine-tagged recombinant proteins in *E. coli* and purified as previously described (Luo et al., 1999; Zhang et al., 2001).

Rat Krp1 was expressed and purified as a fusion protein containing an N-terminal GST-tag using the GST Gene Fusion System (Amersham Biosciences) according to the manufacturer's protocol. The full-length open reading frame of rat Krp1 was PCR amplified as previously described (Spence et al., 2000) and cloned into the *Eco*RI site of the pGex-2TK plasmid. In brief, the pGex-2TK-Krp1 plasmid was transformed into BL21 host *E. coli* cells (Invitrogen). Bacterial cells harboring the expression plasmids were cultured in 2 L of 2× YT medium with 100 μg/ml ampicillin at 37°C. Three hours later the expression of Krp1-GST was induced by the addition of isopropyl thio-β–D-galactoside (IPTG) to a final concentration of 0.2 mM at 24°C followed by an additional 3 hours of incubation. Cells were pelleted after induction by centrifugation at 4000 ***g*** for 15 minutes at 4°C and resuspended in 1/10 culture volume of cellytic B (Sigma) with 10 mg/ml lysozyme, 1 mM PMSF and 0.02 μM leupeptin (Sigma). The cells were then sonicated for 20 seconds in a Branson Sonifier 250 sonicator (Branson Ultrasonics, Danbury, CT) followed by end to end shaking at 4°C for 10 minutes to fully extract the cells. The homogenates were centrifuged at 30,000 ***g*** for 15 minutes at 4°C. GST-tagged Krp1 fusion proteins were purified directly from supernatants using the affinity matrix Glutathione Sepharose 4B (Amersham Biosciences) according to the manufacturer's protocol.

After purification of the recombinant protein, the GST tag was removed by overnight digestion at 22°C with thrombin (Amersham Biosciences) at 10 cleavage units/mg fusion protein in elution buffer (10 mM glutathione, 50 mM Tris-HCl, pH 8.0); cleavage was followed by extensive dialysis against 1 × PBS and column purification on Glutathione Sepharose 4B. The purified Krp1 proteins were found in the flow-through. Purified GST-tagged fusion proteins as well as purified Krp1 proteins after thrombin cleavage were analyzed by gel electrophoresis and immunoblotting as described above using anti-Krp1 polyclonal antibody.

Filamin binding to blotted proteins

Gel overlay binding assays were performed as previously described (Zhang et al., 2001). His-tagged N-RAP recombinant proteins were electrophoresed under denaturing conditions and blotted to PVDF membranes. After washing and blocking, the membranes were incubated overnight at 4°C with 10 μg/ml (0.04 μM total monomer) chicken gizzard filamin (Research Diagnostics, Flanders, NJ) in binding buffer (100 mM KCl, 50 mM Tris-HCl [pH 7.4], 1 mM EGTA, 2 mM $MgCl_2$, 2 mM ATP, 0.3 mM dithiothreitol [DTT], and 0.2% Tween-20). Bound filamin was detected by primary monoclonal antibody against chicken gizzard filamin (Sigma) followed by horseradish peroxidase conjugated anti-mouse antibody (Amersham Biosciences); the primary and secondary antibodies were diluted 1:1000 and 1:2000, respectively, in binding buffer. The ECL western blot system was used for detection of bound antibody (Amersham Biosciences).

Krp1, filamin and α-actinin binding to N-RAP proteins immobilized on Ni-NTA agarose beads

Ni-NTA magnetic agarose beads (Qiagen, Valencia, CA) were used to immobilize histidine-tagged proteins in binding assays performed according to the manufacturer's protocol. In brief, 30 μg of histidine-tagged recombinant proteins (His-N-RAP-SR, His-N-RAP-LIM, His-N-RAP-IB, His-CAT) were incubated with 100 μl of Ni-NTA magnetic agarose beads for 1.5 hours at room temperature under denaturing conditions (8 M urea, 0.1 M NaH_2PO_4, 0.01 M Tris-Cl, 0.005% Tween 20, pH 8.0). The recombinant proteins immobilized on the Ni-NTA matrix were renatured by sequential incubations in 4 M, 2 M, 1 M, and 0 M urea in phosphate buffer (0.1 M NaH_2PO_4, 0.01 M Tris-Cl, 0.005% Tween 20, pH 8.0) over a period of 2 hours. They were then incubated with potentially interacting biomolecules (Krp1, filamin or α-actinin) at final monomer concentrations of 2.5 μg/ml (0.037 μM), 33 μg/ml (0.13 μM) and 33 μg/ml (0.33 μM), respectively. Purified chicken gizzard filamin was purchased from Research Diagnostics (Flanders, NJ) and purified rabbit skeletal muscle α-actinin was purchased from Cytoskeleton (Denver, CO). The binding reactions were incubated with shaking overnight at 4°C in interaction buffer (100 mM KCl, 50 mM Tris-HCl, 1 mM $MgCl_2$, 2 mM ATP, 2.8 mM β-mercaptoethanol, 0.005% Tween-20, 10 mM imidazole, pH 7.5). The Ni-NTA agarose beads were washed 4×15 minutes in interaction buffer to remove unbound proteins and then analyzed by gel electrophoresis and immunoblot detection of Krp1, filamin, or α-actinin. Polyclonal antibody against Krp1 was used followed by horseradish peroxidase conjugated anti-rabbit antibody (Amersham Biosciences); the primary and secondary antibodies were diluted 1:2500 and 1:5000, respectively. Monoclonal antibodies against α-actinin and filamin were used followed by horseradish peroxidase conjugated anti-mouse antibody (Amersham Biosciences); the primary and secondary antibodies were diluted 1:1000 and 1:2000, respectively. The ECL western blot system was used for detecting bound antibody (Amersham Biosciences).

Culture of embryonic chick cardiomyocytes

Primary cardiomyocyte cultures were prepared from 7-10-day-old chick embryos, fixed in 4% formaldehyde, and permeabilized with Nonidet-P-40 as previously described (Carroll and Horowits, 2000). Cells were blocked with 5% normal serum (Sigma) in PBS for 30 minutes. For N-RAP/α-actinin and Krp1/α-actinin double staining, normal goat serum was used; for filamin/α-actinin double staining,

normal donkey serum was used. After blocking, cells were exposed to primary polyclonal antibodies against N-RAP, Krp1, or filamin at a dilution of 1:1000. These antibody exposures were followed by exposure to a monoclonal antibody against sarcomeric α-actinin at a dilution of 1:2000. The N-RAP and Krp1 antibodies were detected using a donkey anti-rabbit FITC-linked secondary antibody at a dilution of 1:100; the filamin antibody was detected using a donkey anti-goat FITC-linked secondary antibody ($F(ab)_2$ fragment; Jackson Immunoresearch Laboratories) at a dilution of 1:100; and the α-actinin antibody was detected using a rhodamine-linked rabbit anti-mouse secondary antibody at a dilution of 1:500. All antibody incubations were for 1 hour at 37°C in PBS. Vectashield (Vector Laboratories, Burlingame, CA) was added to each well to prevent photobleaching. Cardiomyocytes were observed with a Zeiss Axiovert 135 microscope equipped for incident-light fluorescence and phase contrast microscopy using a 63× oil immersion objective with a numerical aperture of 1.25. The appropriate filters for either flourescein or rhodamine fluorescence were used. Images were collected using a Photometrics CoolSnap fx CCD camera (Roper Scientific, Tucson, AZ) interfaced with a Power Macintosh computer.

In order to objectively evaluate co-localization, raw images were composited by storing the rhodamine and fluorescein signals as red and green channels of a single image and then processed using a Macintosh computer. Fluorescent images were inverted and the diffuse background staining of each channel was subtracted with a 2D-rolling ball algorithm with radius set to 50 pixels (5.5 μm) using the public domain NIH Image program [developed at the US National Institutes of Health and available on the NIH website (http://rsb.info.nih.gov/nih-image/)]. After background subtraction, images were inverted and data in each channel were rescaled to occupy the entire dynamic range using Adobe Photoshop software (Adobe Systems, San Jose, CA). Images are presented as separated or overlayed red and green channels. In addition, double staining was further demonstrated by multiplying the background subtracted and rescaled red and green channels to produce a new greyscale image; if a pixel is black (0) in either channel, the result is black in the multiplied image. Therefore, only areas that are fluorescent in both channels are visualized in the multiplied image.

Results

Searching For N-RAP binding partners using the yeast two-hybrid system

We used the yeast two-hybrid technique to identify previously unknown N-RAP binding partners. The previously identified 3.5 kb mouse N-RAP open reading frame was inserted downstream of the LexA DNA-binding domain in the bait vector pHybLex/Zeo to form the bait plasmid. L40 yeast cells transfected with the bait plasmid expressed the full-length LexA-N-RAP fusion protein, which was detected by either anti-N-RAP or anti-LexA antibody on immunoblots (Fig. 1). The anti-LexA antibody also detected the LexA-lamin fusion protein and unfused LexA in yeast cells transfected with the corresponding plasmids (Fig. 1). Bait strain colonies were screened for autoactivation of the *His3* and the *LacZ* reporter genes; bait colonies that exhibited histidine-dependent growth and no β-galactosidase activity were selected for use in the two-hybrid screen for N-RAP binding partners.

The bait strain expressing LexA-N-RAP was transfected with a mouse skeletal muscle cDNA library in which the inserts were expressed as fusion proteins with the B42 transcription

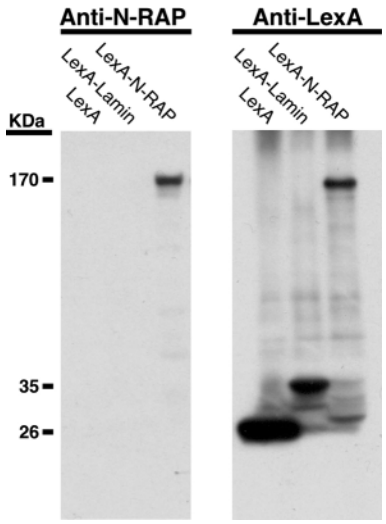

Fig. 1. Lysates from bait L40 yeast strains carrying plasmids encoding the indicated fusion proteins were analyzed for protein expression by immunoblot. LexA fusion proteins were detected using anti-LexA or anti-N-RAP antibodies, as indicated. The results show that the bait strain expressed an intact LexA-N-RAP fusion migrating at 170 kDa, whereas unfused LexA protein migrated at 26 kDa on SDS-PAGE. Also shown are results from a LexA-lamin fusion construct migrating at 35 kDa and used as a negative control for N-RAP binding experiments.

activation domain. Screening 7.2×10^6 cDNA clones led to the identification of 450 double transformants exhibiting β-galactosidase activity and histidine prototrophy. Of these, 90 were randomly selected for further study. PCR and restriction digest analysis of these 90 clones indicated that many were identical, allowing us to create 35 unique groups containing 68 of the clones for further study. The remaining 32 clones were found to contain multiple inserts or no inserts. One or more representatives from each of the 35 groups were tested for specific activation of the reporter genes. Each of the plasmids isolated from these colonies activated both reporter genes when re-introduced into the N-RAP bait strain. However, representatives from 23 of these groups also activated one or both of the reporter genes when introduced into the lamin bait strain, suggesting nonspecific activation. The remaining 12 groups contained 33 clones exhibiting specific positive binding activity for N-RAP in the yeast two-hybrid system. End-sequencing and comparison to the GenBank database identified 15 of these clones as encoding filamin-2 (also called filamin-C or gamma-filamin) (Thompson et al., 2000; van der Ven et al., 2000b; Xie et al., 1998), 11 clones as encoding Krp1 (also called sarcosin) (Spence et al., 2000; Taylor et al., 1998), and four of these clones as encoding α-actinin-3 (Beggs et al., 1992; Mills et al., 2001).

End-sequenceing indicated that the 11 Krp1 clones and the four α-actinin-3 clones isolated all contained the full-length open reading frames of their respective proteins. In contrast, the 15 filamin-2 clones isolated were C-terminal clones of varying lengths (Fig. 2). The shortest filamin clone encodes Ig repeats 20-24 and includes a short hinge region between repeats 23 and 24, demonstrating that N-RAP binds this C-terminal region of filamin.

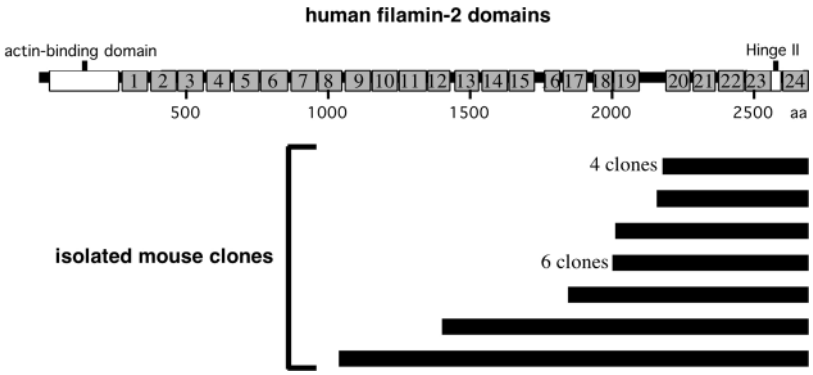

Fig. 2. Schematic representation of human filamin-2 domain structure (Thompson et al., 2000; van der Ven et al., 2000b; Xie et al., 1998), indicating the 24 Ig repeats, the actin binding domain, and the hinge region. The regions encoded by the mouse filamin-2 cDNA clones isolated in the yeast two-hybrid screen for N-RAP binding partners are shown below. Restriction enzyme analysis placed the 15 clones into seven groups of 1-6 clones each, and a total of eight of these clones were end-sequenced. The shortest mouse clones align with Ig repeats 20-24 of the human filamin-2 protein.

Interaction of N-RAP domains with new binding partners in vitro

We used recombinant histidine-tagged N-RAP fragments immobilized on PVDF filters or on magnetic Ni-NTA beads to assay binding activity to the putative binding partners identified in the yeast two-hybrid screen. These assays verified the results of the in vivo screen and identified the specific N-RAP domains mediating the protein-protein interactions.

Fig. 3A illustrates the regions of N-RAP expressed as histidine-tagged fusion proteins for use in binding assays. When muscle α-actinin was incubated with the recombinant N-RAP fragments captured on magnetic Ni-NTA beads, we observed significant binding to the N-RAP LIM domain and to N-RAP-IB; in contrast, no binding was observed to either the N-RAP super repeats or the histidine-tagged CAT proteins (Fig. 3B,C). The results confirm the specificity of α-actinin binding previously observed in a gel overlay assay (Zhang et al., 2001).

Fig. 4 illustrates binding of purified filamin to recombinant N-RAP fragments in both the gel overlay assay (Fig. 4A,B) and the Ni-NTA beads assay (Fig. 4C,D). Both methods demonstrate that filamin binds to the N-RAP super repeats, but does not interact with the N-RAP LIM domain or with N-RAP-IB. The small signals detected for filamin binding to these latter two constructs are similar to those for binding to the His-CAT control proteins, suggesting some nonspecific interaction with the histidine tags present in the recombinant proteins.

Fig. 5 illustrates the purity of the GST-Krp1 fusion protein before and after removal of the GST tag with thrombin; total protein stained with coomassie blue (Fig. 5A) and the immunoblot detected with anti-Krp1 antibody (Fig. 5B) are shown. The results show that purified Krp1 migrates as a single band at the molecular weight predicted from the cDNA sequence. After removal of the GST tag, purified Krp1 was assayed for binding to recombinant N-RAP fragments immobilized on Ni-NTA beads (Fig. 5C,D); the results clearly show that Krp1 binds to N-RAP super repeats and N-RAP-IB, but does not bind the N-RAP LIM domain. We also attempted to assay Krp1 binding to N-RAP fragments using the gel overlay assay. However, control experiments demonstrated that the anti-Krp1 antibody detected the histidine-tagged N-RAP LIM domain, as well as the His-CAT control protein. Because the N-RAP fragments and any binding partners are co-localized on the membrane in the blot overlay assay, the apparent cross-reaction of the antibody with the recombinant tag precluded its use for assaying Krp1 binding to N-RAP fragments.

Localization of N-RAP binding partners during myofibril assembly

We studied the localization of N-RAP and its newly identified binding partners during myofibril assembly in primary cultures of embryonic chick cardiomyocytes. Because α-actinin is an informative marker for all known myofibril precursors as well as for the mature myofibrils, we double stained cardiomyocytes

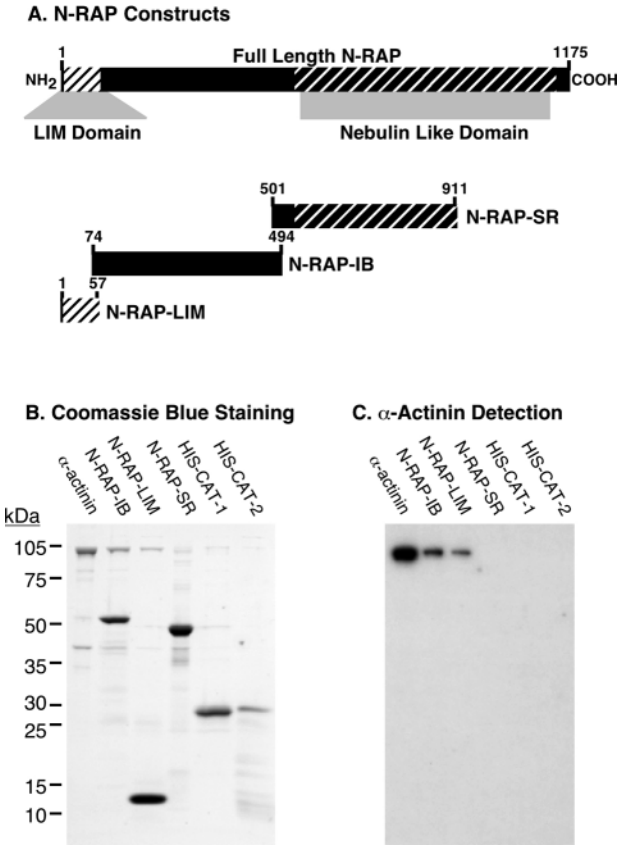

Fig. 3. (A) Schematic diagram showing the domain organization of N-RAP (top), along with the regions of N-RAP expressed as histidine-tagged fusion proteins. Numbers refer to amino acid residues from the full-length mouse N-RAP open reading frame (Luo et al., 1997). (B) α-actinin binding to N-RAP recombinant proteins immobilized on Ni-NTA agarose beads were analyzed by SDS-PAGE. (C) Duplicate loadings were blotted and probed with α-actinin antibody. The antibody specifically detects α-actinin binding to N-RAP-IB and N-RAP-LIM, but does not detect any α-actinin binding to N-RAP-SR or to the His-CAT control proteins.

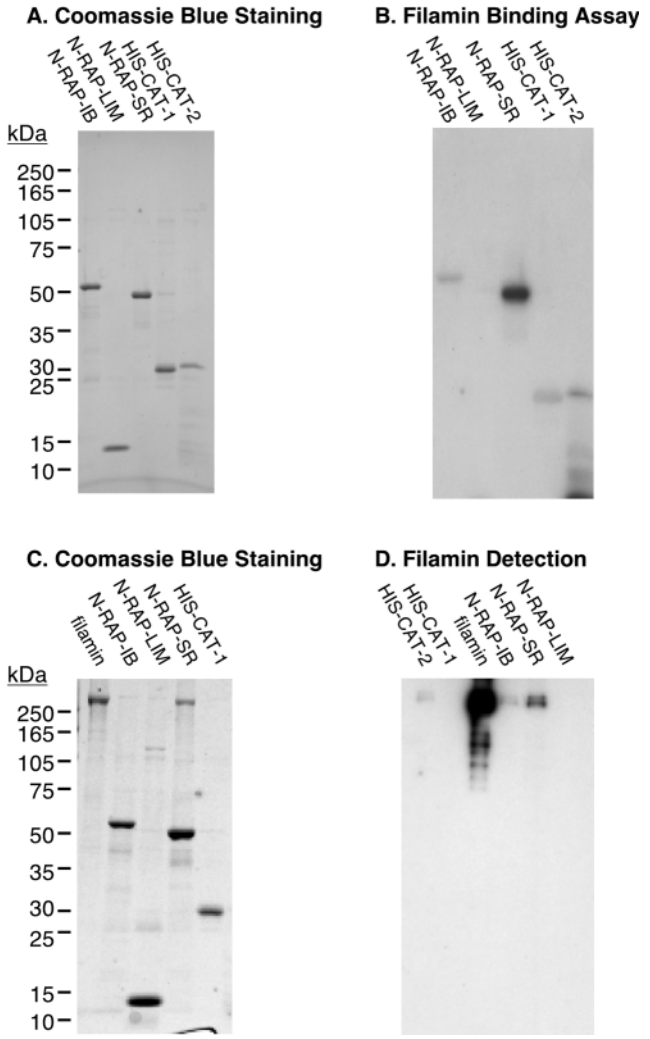

Fig. 4. (A,B) Filamin binding to blotted proteins. Duplicate loadings were used (A) for total protein detection with Coomassie blue and (B) for immunoblot detection of bound filamin. Lanes were loaded with purified proteins as indicated. The histidine-tagged CAT proteins (HIS-CAT-1, HIS-CAT-2) served as negative controls. Significant filamin binding to recombinant N-RAP-SR was observed. (C,D) Filamin binding to N-RAP recombinant proteins immobilized on Ni-NTA agarose beads. Duplicate loadings were used (C) for total protein detection with Coomassie blue and (D) for detection of bound filamin. Significant filamin binding to recombinant N-RAP-SR was observed.

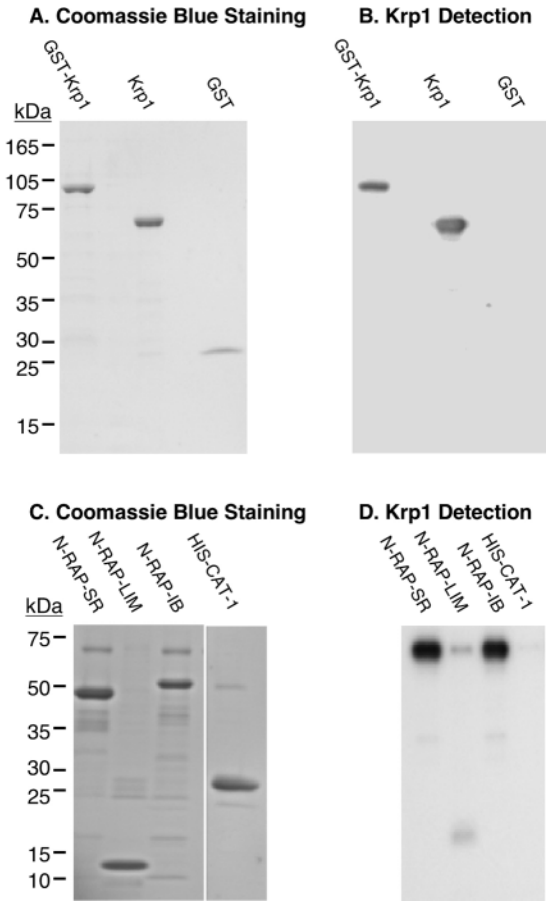

Fig. 5. (A,B) Purified Krp1. Duplicate loadings were used for detection (A) of purified proteins with Coomassie blue and (B) of Krp1 by immunoblot. Lanes were loaded with affinity purified GST-Krp1, and the purified Krp1 and GST following thrombin cleavage. (C,D) Krp1 binding to N-RAP recombinant proteins immobilized on Ni-NTA agarose beads. Duplicate loadings were used (C) for total protein detection with Coomassie blue and (D) for detection of bound Krp1. Significant Krp1 binding to recombinant N-RAP-SR and N-RAP-IB was observed.

for α-actinin and either N-RAP, filamin, or Krp1. Fig. 6A,B show that N-RAP is concentrated along the periphery of the cell where closely spaced α-actinin dots are found. The punctate α-actinin staining in these regions (Fig. 6A) is characteristic of early myofibril precursors (Dabiri et al., 1997; Ehler et al., 1999; Imanaka-Yoshida et al., 1998; Rhee et al., 1994; Rudy et al., 2001). In contrast, the N-RAP staining in these regions is more patchy and diffuse (Fig. 6B); nevertheless, N-RAP staining overlays the punctate α-actinin staining at the periphery of the cardiomyocyte (Fig. 6C,D). The results suggest that N-RAP is a component of the premyofibril that extends beyond the Z-bodies identified by punctate α-actinin staining. N-RAP also appears to be concentrated in regions where narrow sarcomeres appear to be fusing laterally to form broader myofibrils (Fig. 6E-H).

Like N-RAP, filamin is found in large regions of premyofibrils along the cell preiphery, exhibiting a diffuse, mesh-like appearance in contrast with the punctate α-actinin pattern (Fig. 7A-D, asterisks). More centrally located mature myofibrils exhibit broad periodic striations of filamin staining that co-localize with the α-actinin staining in Z-lines (Fig. 7A-D, arrowheads). Some structures are characterized by near continuous α-actinin and filamin staining (Fig. 7 E-H, arrows). As sarcomeres mature and α-actinin spacing increases, filamin staining is still observed between the newly formed Z-lines (Fig. 7E-H, arrowheads). In fully mature regions, filamin staining is restricted to the Z-lines (Fig. 7E-H, asterisks).

Immunoblot analysis demonstrated significant Krp1 protein expression in adult mouse skeletal muscle and primary cultures of embryonic chick cardiomyocytes, but no significant expression in adult mouse heart (Fig. 8). Unlike α-actinin, N-RAP and filamin, Krp1 does not appear to be

localized in the early peripheral myofibril precursors in cultured chick cardiomyocytes. Fig. 9A illustrates a cardiomyocyte with peripheral punctate α-actinin staining as well as more centrally located mature striations of α-actinin. In this cell, Krp1 staining is diffusely distributed in the central region. In more mature cells, Krp1 staining is often seen outlining the periphery of longitudinally oriented myofibrils (Fig. 9B-D). At high magnification, Krp1 staining is often punctate and periodic, exhibiting spacings from 0.5 to 1.0 μm (Fig. 9E, arrowheads). Krp1 is often localized near narrow myofibrils that appear to be fusing laterally with more mature striations (Fig. 9E, arrows). The example in Fig. 9E shows Krp1 staining in the region where the myofibrils appear to be fusing laterally (arrows), but not in a region of the same myofibril that appears to have already undergone this fusion process (asterisk).

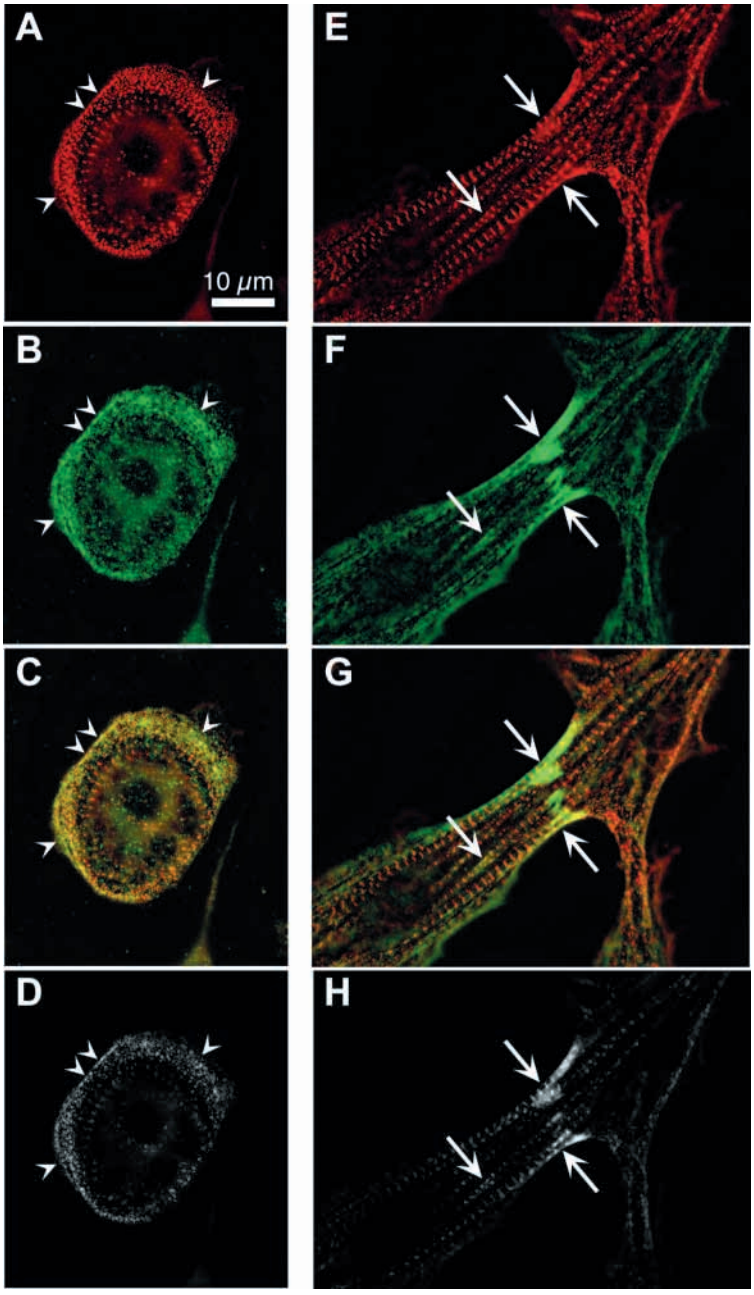

Discussion

New N-RAP binding partners

The results of the two-hyrid screen and in vitro binding assays are summarized in Table 1. An N-RAP bait construct containing the LIM domain, the IB region and the super repeats specifically identified multiple clones encoding filamin-2 (Thompson et al., 2000; van der Ven et al., 2000b; Xie et al., 1998), Krp1 (Spence et al., 2000; Taylor et al., 1998), and α-actinin-3 (Beggs et al., 1992; Mills et al., 2001) as binding partners. In vitro binding studies with recombinant N-RAP domains identified the super repeats as the filamin-binding region of N-RAP, the super repeats and the IB region as Krp1-binding regions, and the IB region and the LIM domain as the α-actinin-binding regions.

Although we tested rabbit muscle α-actinin, rat Krp1, and chicken gizzard filamin for binding to mouse N-RAP, the proteins used are highly conserved between species. For example, the muscle isoforms of α-actinin, α-actinin-2 and α-actinin-3, are functionally redundant (Mills et al., 2001), and are 98% conserved from mice to humans (GenBank accession numbers P35609, Q9JI91, AAC62512, and Q08043). Likewise, rat and human Krp1 are 97% conserved (Spence et al., 2000) (GenBank accession numbers Q9ER30 and O60662). Finally, filamin is encoded by a highly conserved multigene family (van der Flier and Sonnenberg, 2001), and chicken gizzard filamin is 79% similar to human filamin-2 (GenBank accession numbers BAB63943 and AAF80245). Taken together, our results show that α-actinin, Krp1 and filamin can bind specific regions of N-RAP in vitro as well as in a living eukaryotic cell.

α-actinin is the major component of muscle Z-lines (Stromer, 1995), and one of the earliest components to be organized during myofibril assembly (Carroll et al., 2001; Carroll and Horowits, 2000; Dabiri et al., 1997; Ehler et al., 1999; Imanaka-Yoshida et al., 1998; Rhee et al., 1994). It is encoded by a multigene family, and the two isoforms α-actinin-2 and α-actinin-3 are expressed in striated muscle (Mills et al., 2001). Previously, we had shown that N-RAP co-purifies with intercalated disk fractions from adult mouse heart that are enriched for N-cadherin and contain α-actinin, but from which actin and myosin have been extracted (Zhang et al., 2001). We also showed that α-actinin bound both the N-RAP LIM domain and the IB region in a blot overlay assay (Zhang et al., 2001), in agreement with the results of the Ni-NTA magnetic beads assay presented here. In cultured chick cardiomyocytes, α-actinin and N-RAP are concentrated in the earliest

Fig. 6. Cultured embryonic chick cardiomyocytes double-stained for (A,E) α-actinin and (B,F) N-RAP. (C,G) Composite images show both α-actinin staining in red and N-RAP staining in green. (D,H) The multiplied products of the red and green channels emphasize regions containing both N-RAP and α-actinin fluorescence intensity. (A-D) Arrowheads are adjacent to peripheral regions of punctate α-actinin staining that are characteristic of premyofibrils forming near the cell membrane. N-RAP is found in these regions, but is not confined to the α-actinin dots. (E-H) N-RAP is also concentrated in areas where more mature sarcomeres appear to be fusing laterally (arrows).

myofibril precursors that form near the membrane, as well as in more centrally located nascent myofibrils that exhibit almost continuous α-actinin staining (Carroll and Horowits, 2000). In addition, a GFP-tagged N-RAP-IB construct targets to Z-lines (Carroll et al., 2001). Finally, overexpression of GFP tagged N-RAP-IB inhibits myofibril assembly (Carroll et al., 2001). Taken together, the results indicate that the interaction between N-RAP and α-actinin occurs in living cells and is critical for initiating myofibril assembly.

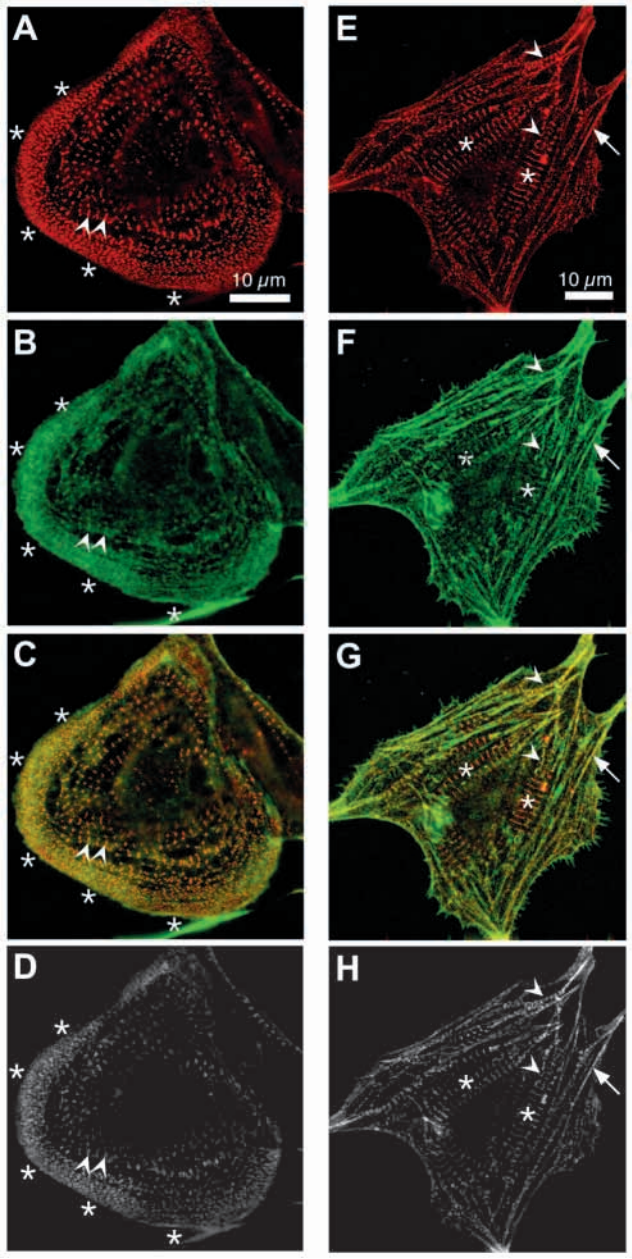

Fig. 7. Cultured embryonic chick cardiomyocytes double-stained for (A,E) α-actinin and (B,F) filamin. Composite images (C,G) show both α-actinin staining in red and filamin staining in green. (D,H) The multiplied products of the red and green channels emphasize regions containing both filamin and α-actinin fluorescence intensity. (A-D) Large regions of premyofibrils are characterized by punctate α-actinin staining along the cell preiphery (asterisks); filamin staining exhibits a more diffuse, mesh-like appearance in these regions. More centrally located mature myofibrils exhibit broad periodic striations of filamin staining that co-localize with the α-actinin staining in Z-lines (arrowheads). (E-H) Some myofibril precursors are characterized by near continuous α-actinin and filamin staining (arrows). As sarcomeres mature and α-actinin spacing increases, filamin staining is still observed between the newly formed Z-lines (arrowheads). In fully mature regions, filamin staining is restricted to the Z-lines (asterisks).

Filamin is also encoded by a multigene family (van der Flier and Sonnenberg, 2001). The predominant striated muscle form is filamin-2, also called filamin-C and gamma-filamin (Thompson et al., 2000; van der Ven et al., 2000b; Xie et al., 1998). As illustrated in Fig. 2, filamin contains an N-terminal actin-binding region followed by a series of 24 Ig repeats; the muscle form also contains one hinge region between repeats 23 and 24. Our yeast two-hybrid results show that N-RAP binds the C-terminal region of filamin that includes the last five repeats and the hinge region (Fig. 2); however, these results do not exclude the possibility that N-RAP binds elsewhere in the filamin molecule as well. We mapped filamin binding to the N-RAP super repeats in vitro. Filamin is found at the Z-lines in mature myofibrils (Bechtel, 1979; Koteliansky et al., 1985; Price et al., 1994; Thompson et al., 2000; van der Ven et al., 2000a; van der Ven et al., 2000b), as well as at the intercalated disks in cardiac tissue and the myotendinous junctions of skeletal muscle (Bechtel, 1979; Koteliansky et al., 1985; van der Ven et al., 2000a). It is also found at the cell periphery, where it is thought to interact with the transmembrane sarcoglycans present in dystrophin-associated complexes (Thompson et al., 2000). As with N-RAP, we observed that filamin co-localizes with premyofibrils and non-striated nascent myofibrils during myofibril assembly (Fig. 7), in agreement with previous findings (van der Ven et al., 2000a). Although exogenous filamin incorporates into assembling Z-bodies as well as mature Z-bands in living cardiomyocytes (Mittal et al., 1987), we found that α-

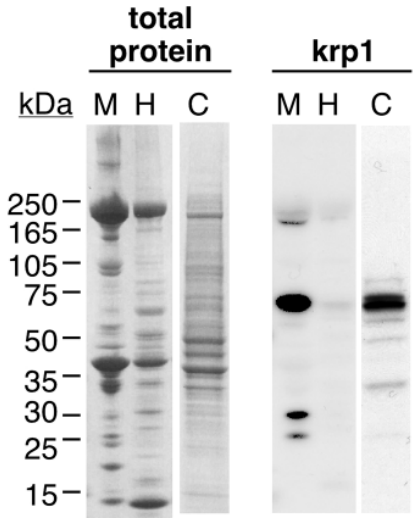

Fig. 8. Krp1 expression in mouse muscle and chick cardiomyocytes. Duplicate loadings were used (left) for detection of total proteins with coomassie blue and (right) of Krp1 by immunoblot. Lanes were loaded with total homogenates from mouse skeletal muscle (M) and heart (H), as well as lystates from cultured embryonic chick cardiomyocytes (C). The Krp1 antibody specifically detects a 68 kDa band in mouse skeletal muscle and chick cardiomyocytes, but no Krp1 is detected in mouse heart tissue.

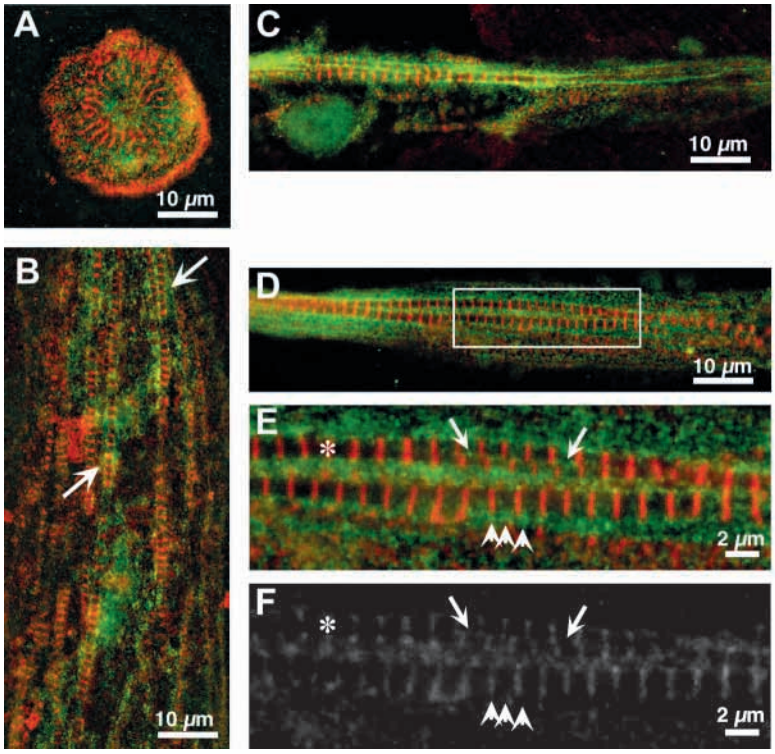

Fig. 9. Cultured embryonic chick cardiomyocytes double-stained for α-actinin (red) and Krp1 (green). (A) Krp1 staining is diffuse during early stages of myofibril assembly. (B-D) In more mature cells, Krp1 often outlines the periphery of longitudinally oriented myofibrils (arrows). The boxed area in (D) is shown at higher magnification in (E), and (F) shows the multiplied product of the red and green channels, which emphasizes regions containing both α-actinin and Krp1 fluorescence intensity. (E,F) Krp1 staining is often punctate and periodic, exhibiting spacings from 0.5 to 1.0 μm (arrowheads). This example also shows Krp1 localized near narrow myofibrils that appear to be fusing laterally with more mature striations (arrows), but no Krp1 staining in a region of the same myofibril that appears to have already undergone this fusion process (asterisk).

actinin appears to organize into striations before filamin becomes restricted to the Z-lines (Fig. 7).

Krp1 (kelch related protein 1) (Spence et al., 2000), also called sarcosin (Taylor et al., 1998), is a member of the kelch repeat superfamily of proteins (Adams et al., 2000). It contains five C-terminal kelch repeats as well as an N-terminal BTB/POZ domain (Spence et al., 2000). The Krp1 transcript is highly expressed in human and rat skeletal muscle (Spence et al., 2000; Taylor et al., 1998), as well as in fibroblasts transformed with FBR murine sarcoma virus (FBR cells) (Spence et al., 2000). We detected significant levels of Krp1 in embryonic chick cardiomyocytes as well as in adult mouse skeletal muscle, but little or no Krp1 in adult mouse hearts. Many kelch proteins bind actin and modify actin organization (Adams et al., 2000), and in FBR cells Krp1 is found in pseudopodia at the tips of actin filaments (Spence et al., 2000). We mapped Krp1 binding to the N-RAP super repeats and the N-RAP IB region in vitro. In cultured embryonic chick cardiomyocytes, we found Krp1 at the periphery of mature myofibrils that appeared to be joining laterally with narrow myofibrils (Fig. 9). This lateral fusion process is responsible for transforming myofibril precursors into mature myofibrils with broad Z-lines (Dabiri et al., 1997). The results suggest that Krp1 is involved late in myofibril assembly, and may catalyze the lateral fusion of myofibril precursors.

Implications for myofibril assembly

Previously, we proposed that N-RAP functions as an organizing center during the first steps of myofibril assembly, with the N-RAP LIM domain targeting to a membrane-associated complex, the N-RAP IB region involved in binding α-actinin, and the N-RAP super repeats promoting actin polymerization and appropriate integration with α-actinin (Carroll et al., 2001). This model is strongly supported by more recent work showing that overexpression of an N-RAP deletion mutant that is missing the super repeats disrupts actin assembly while permitting normal Z-line assembly (Carroll et al., 2002). However, details regarding essential steps before and after these key events remain to be elucidated.

Importantly, the identity of the components responsible for tethering the initial premyofibril assembly to the membrane remains unknown. α-Actinin (Figs 6, 7 and 9) (Carroll et al., 2001; Carroll and Horowits, 2000; Dabiri et al., 1997; Ehler et al., 1999; Imanaka-Yoshida et al., 1998; Rhee et al., 1994), N-RAP (Fig. 6) (Carroll and Horowits, 2000), and filamin (Fig. 7) (van der Ven et al., 2000a) are components of the earliest myofibril precursors near the cell periphery, and their known binding partners identify candidates for the initial integral membrane anchor in myofibril assembly. These candidates include integrins, sarcoglycans, and cadherins: α-actinin (Otey et al., 1990) and filamin (Goldmann, 2000; Loo et al., 1998; Pfaff et al., 1998) can directly bind the transmembrane β-integrins, whereas N-RAP may link to β-integrins by binding talin (Luo et al., 1999). Muscle filamin can also bind sarcoglycans (Thompson et al., 2000), whereas α-actinin may be coupled to the transmembrane cadherins through its interaction with catenins (Kemler, 1993; Knudsen et al., 1995; Nieset et al., 1997).

After the initial α-actinin/actin assembly is formed, the complex moves toward the cell interior, N-RAP leaves the complex, and the structures fuse laterally to form mature Z-

Table 1. New N-RAP binding partners

	Two-hybrid screen	In vitro binding assay		
Binding partner	# Clones	N-RAP-SR	N-RAP-IB	N-RAP-LIM
Filamin	15	+	–	–
Krp1 (Sarcosin)	11	+	+	–
α-Actinin	4	–	+	+

lines (Carroll et al., 2001). Filamin also becomes restricted to the Z-lines during this time (Fig. 7). The findings that Krp1 localizes at the periphery of laterally fusing myofibrils (Fig. 9), that Krp1 has kelch repeats that may constitute multiple actin-binding domains (Spence et al., 2000), and that Krp1 binds the N-RAP super repeats and the N-RAP IB region (Fig. 5), and that these N-RAP domains target to structures that contain actin and α-actinin, respectively (Carroll et al., 2001), are all consistent with a role for Krp1 in the final steps of myofibril maturation. We propose that Krp1 interaction with actin and N-RAP catalyzes the dissociation of N-RAP from the premyofibril complex and allows the lateral fusion of these structures to form mature myofibrils. Experiments to test this hypothesis will bring us closer to understanding the molecular mechanisms involved in myofibril assembly.

Bradford Ozanne was supported by Cancer Research UK.

References

Adams, J., Kelso, R. and Cooley, L. (2000). The kelch repeat superfamily of proteins: propellers of cell function. *Trends Cell Biol.* **10**, 17-24.

Bartel, P. L. and Fields, S. (1995). Analyzing protein-protein interactions using two-hybrid system. *Methods Enzymol.* **254**, 241-263.

Bechtel, P. J. (1979). Identification of a high molecular weight actin-binding protein in skeletal muscle. *J. Biol. Chem.* **254**, 1755-1758.

Beggs, A. H., Byers, T. J., Knoll, J. H., Boyce, F. M., Bruns, G. A. and Kunkel, L. M. (1992). Cloning and characterization of two human skeletal muscle alpha-actinin genes located on chromosomes 1 and 11. *J. Biol. Chem.* **267**, 9281-9288.

Carroll, S. L., Herrera, A. H. and Horowits, R. (2001). Targeting and functional role of N-RAP, a nebulin-related LIM protein, during myofibril assembly in cultured chick cardiomyocytes. *J. Cell Sci.* **114**, 4229-4238.

Carroll, S. L., Herrera, A. H. and Horowits, R. (2002). N-RAP super repeats organize actin filaments during myofibril assembly in cultured chick cardiomyocytes. *Mol. Biol. Cell* **13**, 35a.

Carroll, S. L. and Horowits, R. (2000). Myofibrillogenesis and formation of cell contacts mediate the localization of N-RAP in cultured chick cardiomyocytes. *Cell Motil. Cytoskeleton* **47**, 63-76.

Dabiri, G. A., Turnacioglu, K. K., Sanger, J. M. and Sanger, J. W. (1997). Myofibrillogenesis visualized in living embryonic cardiomyocytes. *Proc. Natl. Acad. Sci. USA* **94**, 9493-9498.

Ehler, E., Horowits, R., Zuppinger, C., Price, R. L., Perriard, E., Leu, M., Caroni, P., Sussman, M., Eppenberger, H. M. and Perriard, J. C. (2001). Alterations at the intercalated disk associated with the absence of muscle LIM protein. *J. Cell Biol.* **153**, 763-772.

Ehler, E., Rothen, B. M., Hämmerle, S. P., Komiyama, M. and Perriard, J.-C. (1999). Myofibrillogenesis in the developing chicken heart: assembly of the z-disk, m-line and thick filaments. *J. Cell Sci.* **112**, 1529-1539.

Goldmann, W. H. (2000). Kinetic determination of focal adhesion protein formation. *Biochem. Biophys. Res. Commun.* **271**, 553-557.

Herrera, A. H., Elzey, B., Law, D. J. and Horowits, R. (2000). Terminal regions of mouse nebulin: sequence analysis and complementary localization with N-RAP. *Cell Motil. Cytoskeleton* **45**, 211-222.

Holtzer, H., Hijikata, T., Lin, Z. X., Zhang, Z. Q., Holtzer, S., Protasi, F., Franzini-Armstrong, C. and Sweeney, H. L. (1997). Independent assembly of 1.6 microns long bipolar MHC filaments and I-Z- I bodies. *Cell Struct. Funct.* **22**, 83-93.

Imanaka-Yoshida, K., Knudsen, K. A. and Linask, K. K. (1998). N-cadherin is required for the differentiation and initial myofibrillogenesis of chick cardiomyocytes. *Cell Motil. Cytoskeleton* **39**, 52-62.

Kemler, R. (1993). From cadherins to catenins: cytoplasmic protein interactions and regulation of cell adhesion. *Trends Genet.* **9**, 317-321.

Knudsen, K. A., Soler, A. P., Johnson, K. R. and Wheelock, M. J. (1995). Interaction of alpha-actinin with the cadherin/catenin cell-cell adhesion complex via alpha-catenin. *J. Cell Biol.* **130**, 67-77.

Koteliansky, V. E., Shirinsky, V. P., Gneushev, G. N. and Chernousov, M. A. (1985). The role of actin-binding proteins vinculin, filamin, and fibronectin in intracellular and intercellular linkages in cardiac muscle. *Adv. Myocardiol.* **5**, 215-221.

Loo, D. T., Kanner, S. B. and Aruffo, A. (1998). Filamin binds to the cytoplasmic domain of the beta1-integrin. Identification of amino acids responsible for this interaction. *J. Biol. Chem.* **273**, 23304-23312.

Luo, G., Herrera, A. H. and Horowits, R. (1999). Molecular interactions of N-RAP, a nebulin-related protein of striated muscle myotendon junctions and intercalated disks. *Biochemistry* **38**, 6135-6143.

Luo, G., Zhang, J. Q., Nguyen, T. P., Herrera, A. H., Paterson, B. and Horowits, R. (1997). Complete cDNA sequence and tissue localization of N-RAP, a novel nebulin-related protein of striated muscle. *Cell Motil. Cytoskeleton* **38**, 75-90.

Mills, M., Yang, N., Weinberger, R., Vander Woude, D. L., Beggs, A. H., Easteal, S. and North, K. (2001). Differential expression of the actin-binding proteins, alpha-actinin-2 and -3, in different species: implications for the evolution of functional redundancy. *Hum. Mol. Genet.* **10**, 1335-1346.

Mittal, B., Sanger, J. M. and Sanger, J. W. (1987). Binding and distribution of fluorescently labeled filamin in permeabilized and living cells. *Cell Motil. Cytoskeleton* **8**, 345-359.

Moncman, C. L. and Wang, K. (1995). Nebulette: a 107 kD nebulin-like protein in cardiac muscle. *Cell Motil. Cytoskeleton* **32**, 205-225.

Moncman, C. L. and Wang, K. (1999). Functional dissection of nebulette demonstrates actin binding of nebulin-like repeats and Z-line targeting of SH3 and linker domains. *Cell Motil. Cytoskeleton* **44**, 1-22.

Nieset, J. E., Redfield, A. R., Jin, F., Knudsen, K. A., Johnson, K. R. and Wheelock, M. J. (1997). Characterization of the interactions of alpha-catenin with alpha-actinin and beta-catenin/plakoglobin. *J. Cell Sci.* **110**, 1013-1022.

Otey, C. A., Pavalko, F. M. and Burridge, K. (1990). An interaction between alpha-actinin and the beta 1 integrin subunit in vitro. *J. Cell Biol.* **111**, 721-729.

Pfaff, M., Liu, S., Erle, D. J. and Ginsberg, M. H. (1998). Integrin beta cytoplasmic domains differentially bind to cytoskeletal proteins. *J. Biol. Chem.* **273**, 6104-6109.

Price, M. G., Caprette, D. R. and Gomer, R. H. (1994). Different temporal patterns of expression result in the same type, amount, and distribution of filamin (ABP) in cardiac and skeletal myofibrils. *Cell Motil. Cytoskeleton* **27**, 248-261.

Rhee, D., Sanger, J. M. and Sanger, J. W. (1994). The premyofibril: evidence for its role in myofibrillogenesis. *Cell Motil. Cytoskeleton* **28**, 1-24.

Rudy, D. E., Yatskievych, T. A., Antin, P. B. and Gregorio, C. C. (2001). Assembly of thick, thin, and titin filaments in chick precardiac explants. *Dev. Dyn.* **221**, 61-71.

Schultheiss, T., Lin, Z. X., Lu, M. H., Murray, J., Fischman, D. A., Weber, K., Masaki, T., Imamura, M. and Holtzer, H. (1990). Differential distribution of subsets of myofibrillar proteins in cardiac nonstriated and striated myofibrils. *J. Cell Biol.* **110**, 1159-1172.

Spence, H. J., Johnston, I., Ewart, K., Buchanan, S. J., Fitzgerald, U. and Ozanne, B. W. (2000). Krp1, a novel kelch related protein that is involved in pseudopod elongation in transformed cells. *Oncogene* **19**, 1266-1276.

Stromer, M. H. (1995). Immunocytochemistry of the muscle cell cytoskeleton. *Microsc. Res. Tech.* **31**, 95-105.

Taylor, A., Obholz, K., Linden, G., Sadiev, S., Klaus, S. and Carlson, K. D. (1998). DNA sequence and muscle-specific expression of human sarcosin transcripts. *Mol. Cell. Biochem.* **183**, 105-112.

Thompson, T. G., Chan, Y. M., Hack, A. A., Brosius, M., Rajala, M., Lidov, H. G., McNally, E. M., Watkins, S. and Kunkel, L. M. (2000). Filamin 2 (FLN2): A muscle-specific sarcoglycan interacting protein. *J. Cell Biol.* **148**, 115-126.

van der Flier, A. and Sonnenberg, A. (2001). Structural and functional aspects of filamins. *Biochim. Biophys. Acta* **1538**, 99-117.

van der Ven, P. F., Obermann, W. M., Lemke, B., Gautel, M., Weber, K. and Furst, D. O. (2000a). Characterization of muscle filamin isoforms suggests a possible role of gamma-filamin/ABP-L in sarcomeric Z-disc formation. *Cell Motil. Cytoskeleton* **45**, 149-162.

van der Ven, P. F., Wiesner, S., Salmikangas, P., Auerbach, D., Himmel, M., Kempa, S., Hayess, K., Pacholsky, D., Taivainen, A., Schroder, R. et al. (2000b). Indications for a novel muscular dystrophy pathway. gamma-filamin, the muscle-specific filamin isoform, interacts with myotilin. *J. Cell Biol.* **151**, 235-248.

Xie, Z., Xu, W., Davie, E. W. and Chung, D. W. (1998). Molecular cloning of human ABPL, an actin-binding protein homologue. *Biochem. Biophys. Res. Commun.* **251**, 914-919.

Zhang, J. Q., Elzey, B., Williams, G., Lu, S., Law, D. J. and Horowits, R. (2001). Ultrastructural and biochemical localization of N-RAP at the interface between myofibrils and intercalated disks in the mouse heart. *Biochemistry* **40**, 14898-14906.